

# **Flat Plate Radiometer Subsystem For ITOS Spacecraft**

**Principal Investigator**

**Robert J. Parent**

**Contributors**

**Robert P. Wollersheim**

**Robert M. Dombroski**

**Space Science and Engineering Center**

**University of Wisconsin**

**Madison, Wisconsin**

**May 1972**

Space Science and Engineering Center  
University of Wisconsin  
Madison, Wisconsin

FLAT PLATE RADIOMETER SUBSYSTEM FOR ITOS SPACECRAFT

Final Technical Report

on

E-73-68-(N)

October, 1967 - June, 1972

The research in this document has been supported in whole by the National Oceanographic and Atmospheric Administration, National Environmental Satellite Service.

May, 1972

## TABLE OF CONTENTS

	Page
A. INTRODUCTION	1
1. General	1
2. Objective	1
3. Earth-Oriented Operation	3
4. FPR Operation	5
5. Performance	5
B. SENSORS	7
1. Sensor Spectral Response	7
2. RE Sensors	7
3. TF Sensors	8
4. Other Sensors	9
5. Cone Shielded Sensors for S/N 005 FPR	9
C. FPR ELECTRONICS	11
1. Function	11
2. Accuracy and Stability	16
3. Power	21
4. RFI and Compatibility	22
5. Modifications to S/N 005 FPR	22
D. MECHANICAL DESIGN	22
1. Physical Requirements	22
2. Design	24
3. Fabrication	27
E. THERMAL DESIGN	27
1. General	27
2. RE Sensor Mount	29
3. TF Sensor Mount	30
4. Spacecraft Heat Loss	30
5. Flight Temperature Prediction	30
F. SENSOR CALIBRATION	34
1. In-Air Calibration	34
2. Vacuum Calibration	36
3. RE Loss Measurement	36
G. PERFORMANCE AND RESULTS	36
1. Operation Summary	36
2. Results	37
3. Data Reduction and Analysis	43

## LIST OF FIGURES

Figure	Page
1. Flat Plate Radiometer Orientation	2
2. Flat Plate Radiometer	3
3. Flat Plate Radiometer, Solar Illumination	4
4. Flat Plate Radiometer, Basic Block Diagram	6
5. Spectral Regions Used by FPR	8
6. Directional Spectral Emissivity of FPR Sensor Disk Surfaces	9
7. Flat Plate Radiometer Sensor Assembly, Exploded View	10
8. Flat Plate Radiometer, Function Block Diagram	12
9. Flat Plate Radiometer Timing Diagram	13
10. Flat Plate Radiometer Logic Timing Diagram	14
11. ITOS Flat Plate Radiometer Board 1	17
12. ITOS Flat Plate Radiometer Board 2	18
13. ITOS Flat Plate Radiometer Board 3	19
14. ITOS Flat Plate Radiometer Board 4	20
15. Flat Plate Radiometer Outline Drawing	23
16. Flat Plate Radiometer Instrument Package	25
17. View of Flat Plate Radiometer Electronics	26
18. Honeycomb Panel Construction	28
19. RE Sensor-Cooling Mirror Geometry	29
20. Flat Plate Radiometer Mounted on Spacecraft	31
21. Analytical Thermal Schematic	32



Figure	Page
22. Thermal Vacuum Test Set-up	33
23. Typical RE Sensor In-Air Calibration Data Plot	38
24. Typical TF Sensor Vacuum Calibration Data Plot	39
25. Typical RE Sensor Flight Data	40
26. Typical TF Sensor Flight Data	41

## LIST OF TABLES

Table	Page
1. FPR Word Content	15
2. Thermal-Vacuum Data Summary	33
3. Average Difference Between Test and Analytical Model Temperatures	34
4. Calculated RE Mount Transient Temperatures	35
5. FPR Unit History Summary	37

## A. INTRODUCTION

### 1. General

The Flat Plate Radiometer (FPR) subsystems have been designed for the measurement of the earth's heat balance from the vantage point of the ITOS earth-oriented platform.

The FPR was designed and built by the University of Wisconsin Space Science and Engineering Center for the National Oceanic and Atmospheric Administration/National Environmental Satellite Service under Contract E-73-68(N).

The entire FPR is contained in a single enclosure which is mounted exterior to and on the spacecraft earth-oriented surface. (See Figure 1.) The FPR package configuration is shown in Figure 2. The major components are the housing, which is constructed of sandwich honeycomb, four sensors, a cooling mirror for one pair of sensors, and the electronics.

### 2. Objective

The FPR is designed to measure the heat budget of the earth by determining the total thermal radiation from the earth by means of a broad spectral response "black" sensor and essentially only the long wave thermal radiation by means of a "white" sensor that rejects most of the solar. The incoming solar radiation is considered to be calculable and is not measured directly. Thus, with the incoming solar, reflected solar (albedo) plus self-thermal radiation (long wave) and long wave alone known, the radiation budget can be computed.

Since the spectral emissivity of the sensor surfaces, particularly the white surface, may change with time, a means of in-flight calibration in the long-wave region has been included. One set of black and white sensors can be physically rotated to view a black cavity at a known temperature. Thus, it should be possible to determine the emissivity of the sensor surfaces throughout the life of the instrument.

Another requirement on the system was that a set of flat plate sensors with hemispherical field of view and identical to those flown on the ESSA series of spinning spacecraft be incorporated to provide continuity of measurement.

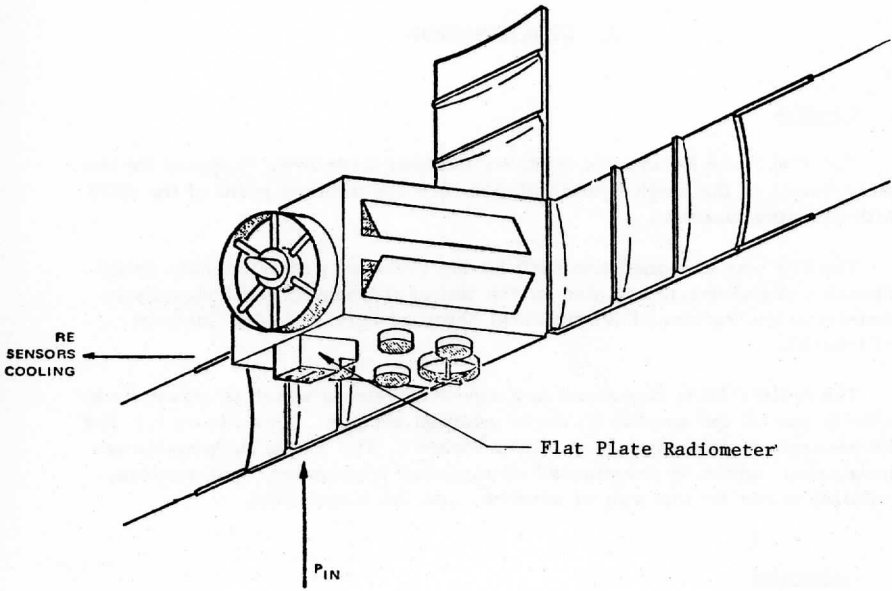


Figure 1. Flat Plate Radiometer Orientation. (Figure by permission of NOAA/RCA.)

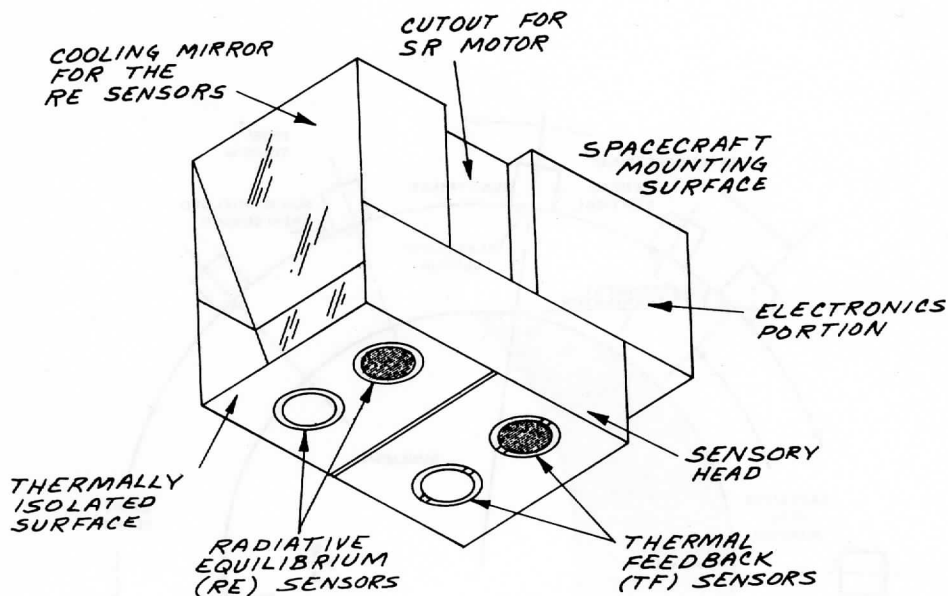


Figure 2. Flat Plate Radiometer

### 3. Earth-Oriented Operation

In the case of the spinning spacecraft such as ESSA, the input to the flat plate sensors consisted of direct solar, reflected solar and earth self-radiation when the spacecraft was in the sun, to a minimum of earth radiation only when in the middle of eclipse. In all cases the sensor input was time-averaged by the sensor over each revolution of the spacecraft, as well as spatially averaged.

For oriented operation averaging is done only in a spatial sense due to spacecraft motion along the orbit. For most of the orbit, the sensors are not exposed to direct solar due to the shielding provided by the spacecraft or the earth; see Figure 3. However, for two intervals each orbit, about  $21^\circ$ , between the terminator and eclipse, the sensors are exposed to direct solar in varying degree. The direct solar contribution is large and tends to mask the variations in reflected solar and long wave radiation one desires to measure. The system has been designed with sufficient dynamic range to handle the direct solar.

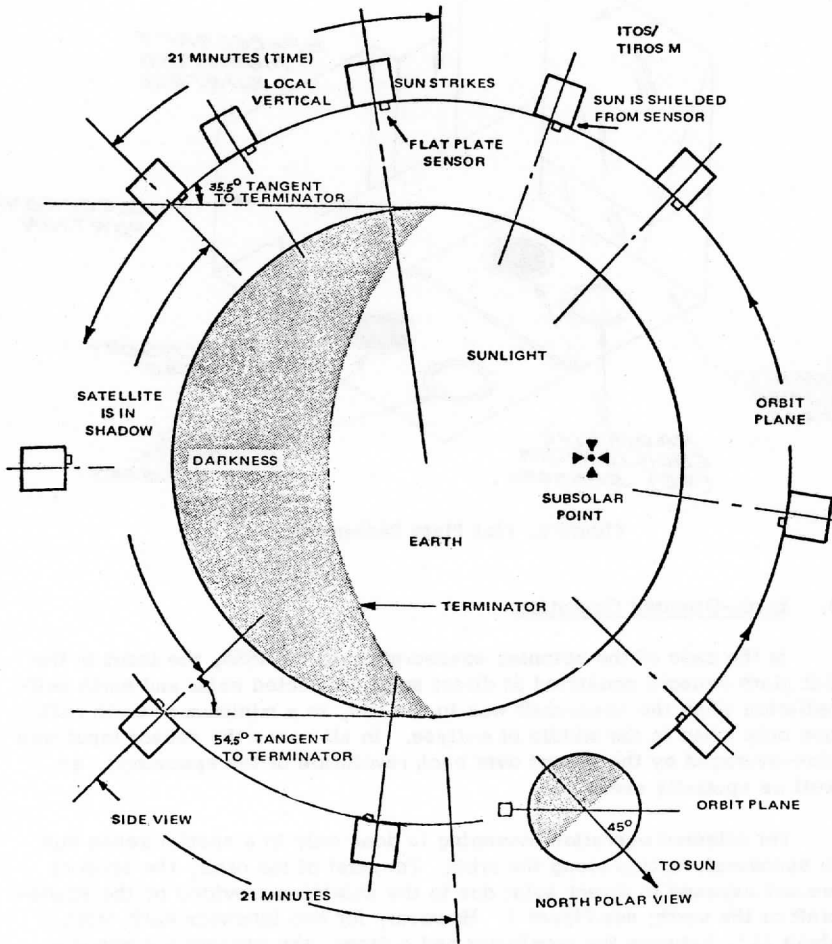


Figure 3. Flat Plate Radiometer, Solar Illumination (3 PM Orbit). (Figure by permission of NOAA/RCA.)

#### 4. FPR Operation

System operation will be described briefly with the aid of the block diagram of Figure 4.

Two types of transducers are used. For one, thermistors (thermally sensitive resistors) are used as the sensing elements for temperature determination. For the other, the sensing is done by measuring the electrical energy required to maintain the temperature of a thermal radiation receiver constant against variation in the received energy. This process will be referred to as "thermal feedback" or TF.

The variable resistance transducer type includes the radiative equilibrium (RE) thermal radiation sensors and others for the determination of auxiliary temperatures. These are time division multiplexed to a common resistance-to-frequency converter, the output of which is gated to a counter for a fixed time interval to produce a count proportional to the input frequency. After each gating and counting cycle the content of the counter is transferred to a shift register and shifted out during the next accumulation cycle. The serial digital output is formatted and recorded on magnetic tape by a subsystem on board the spacecraft.

The energy or thermal feedback, TF, type sensors require individual control circuits to maintain the radiation receiver surface at constant temperature. Temperature control is accomplished by feedback control of the frequency of a train of equal energy pulses to a heating element in the sensor. Measurement in this case is made by sampling (multiplexing) the frequency sources with the TF select gate rather than switching the sensor elements. The time gating, counting, transfer and shift out of the data is the same as for the other sensors.

All of the timing comes from the control logic which in turn receives master timing from the spacecraft.

#### 5. Performance

In all, five FPR subsystems were built and delivered, including one engineering unit and four flight units. Two units were launched and performed as expected, until failure of the spacecraft data collection and storage system terminated operation.

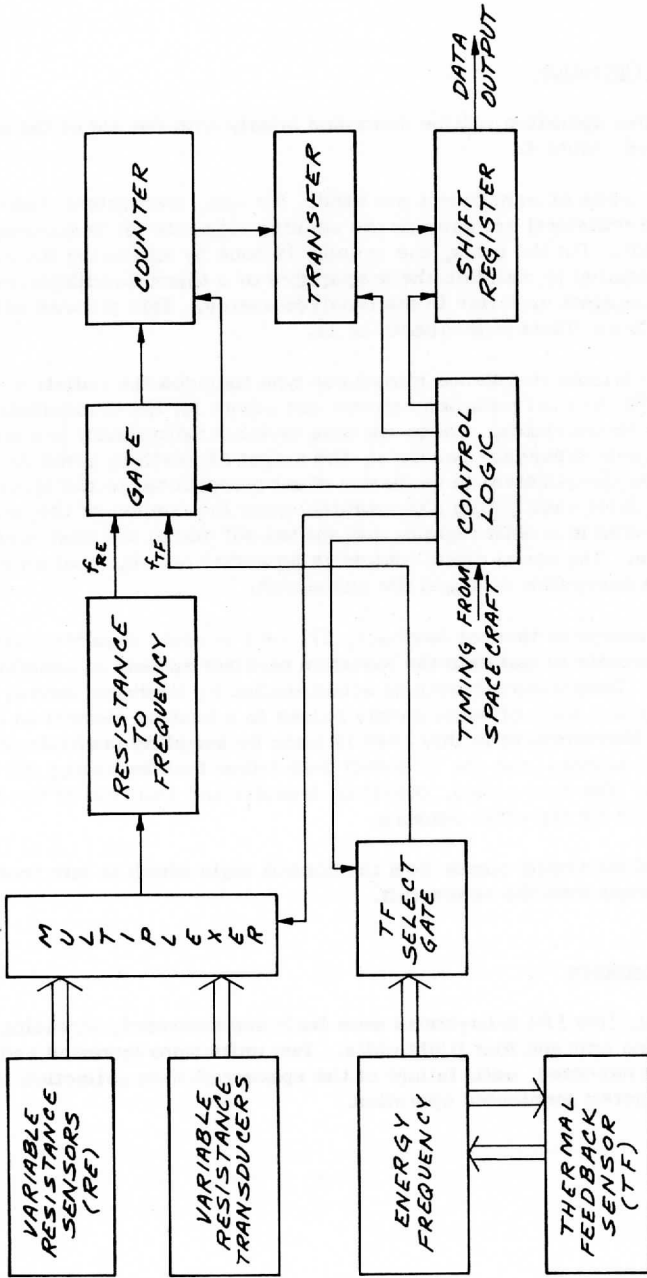


Figure 4. Flat Plate Radiometer, Basic Block Diagram



## B. SENSORS

The sensor complement of the FPR consists of four sensors for measuring incident radiation and eight others for measuring temperature directly.

### 1. Sensor Spectral Response

The determination of the heat budget of the earth requires the measurement of the incoming solar, reflected solar (albedo) and self-emitted long-wave (IR) earth radiation. The solar and long-wave components as such are also required. Independent measurement is simplified by the fact that the solar and IR spectra have essentially no overlap. See Figure 5.

Spectral separation is accomplished in the FPR by use of two sensors with different spectral response. One sensor is "black" and has an essentially constant spectral response from  $< 0.3 \mu\text{m}$  to  $> 30 \mu\text{m}$  and so absorbs solar and long-wave equally. See Figure 6. The black surface is coated with 3-M 400 black paint. The other is "white" in the solar and hence reflects most of the solar but has high absorptivity in the long-wave from about  $7 \mu\text{m}$  to  $> 30 \mu\text{m}$  and so appears black in this spectral region (Figure 6). The white surface is anodized aluminum.

Thus, total radiation is measured by the black sensor, essentially only long-wave by the white sensor and the solar is obtained by subtracting the long-wave (white) from the total (black).

### 2. RE Sensors

Two of the radiation sensors, one black and one white, are of the "radiative equilibrium" type. The sensor consists basically of a thin aluminum disk which can absorb and emit radiation from one side but which is effectively isolated both radiatively and conductively otherwise. See exploded view of sensor, Figure 7. Ideally, then, the disk must come to an equilibrium temperature such that the absorbed and emitted power are equal, hence the name "radiative equilibrium." The temperature of the disk is measured using thermistors to give the emitted power per unit area  $w_e = \epsilon \sigma T^4$  which must equal the absorbed incident power per unit area, or  $\alpha H$ , where  $H$  is the irradiance at the sensor, the quantity to be measured.

Since the isolation of the sensor disk from its supporting mount structure is not perfect, some correction, which is a function of disk and mount temperatures, must be made. In order to do this, mount temperature measurement is provided for in the system.

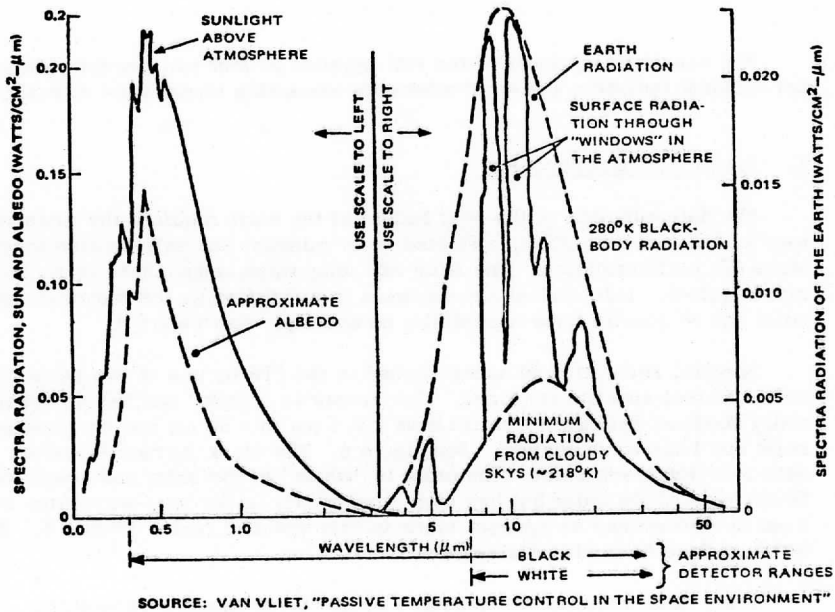


Figure 5. Spectral Regions Used by the Flate Plate Radiometer. (Figure by permission of NOAA/RCA.)

### 3. TF Sensors

The other two radiation sensors, one black and one white, are of the "thermal feedback" type. The basic construction of the TF sensors is the same as that for the RE sensors, a thin aluminum disk effectively isolated both radiatively and conductively except for its active surface.

The operation of the sensors is quite different, however. Rather than letting the sensor come to radiative equilibrium as for the RE sensors, the sensor disk is held at a fixed temperature by an active control circuit. As the radiation incident on the sensor changes, the change in power from the control circuit to a heating element on the sensor disk to maintain constant disk temperature must be equal in magnitude but opposite in sign. Electrical power is fed back to the sensor and converted to heat to maintain

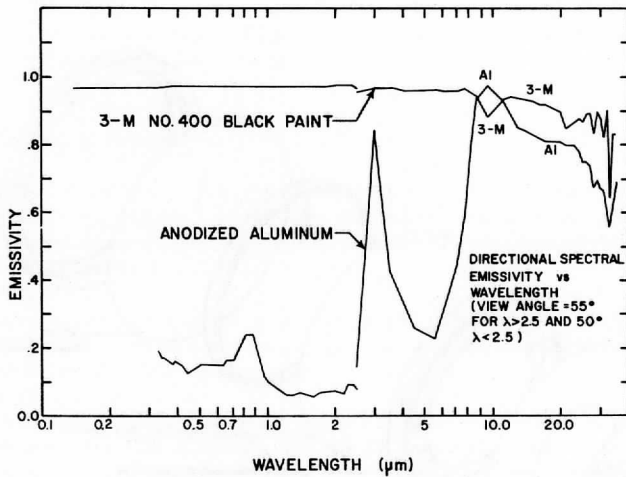


Figure 6. Directional Spectral Emissivity of Plate Radiometer Sensor Disk Surfaces

constant temperature, hence the term "thermal feedback." The absorbed power in this case is measured indirectly by measuring the electric power.

Again, isolation of the active sensor from its mounting structure is not perfect and so the mount temperature is measured and correction made to the data when processed.

Although the control system should hold the sensor disk at constant temperature, its temperature is measured as a check on operation.

#### 4. Other Sensors

Thermistors are used as sensing elements for determining the temperature of the RE and TF disks and mounts, the TF calibration hemispheres and the electronics.

#### 5. Cone Shielded Sensors for S/N 005 FPR

Reference to Figure 3 will show that twice during the orbit, when the spacecraft is between the terminator and eclipse, direct solar radiation

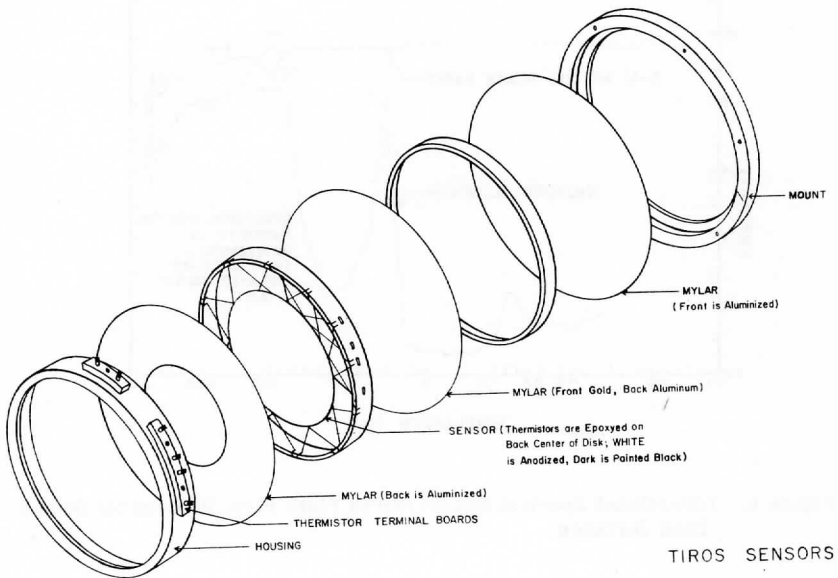


Figure 7. Flat Plate Radiometer Sensor Assembly, Exploded View.

strikes the FPR sensors. The direct component is large in magnitude and tends to override the normal component from the earth. In an effort to prevent direct solar contamination, two RE type sensors were mounted in cone shields. The cones are designed to allow practically full earth view by the sensors but not allow direct solar input, even when the spacecraft crosses the tangent to the terminator.

Two cone shielded sensors, one white and one black, were substituted for the TF sensors on the S/N 005 package which was mounted on the ITOS-B S/C. Since the spacecraft failed to achieve orbit, no flight performance data is available for this sensor configuration.

## C. FPR ELECTRONICS

### 1. Function

Figure 8 is a functional diagram of the system. The FPR electronics is controlled by spacecraft-provided clock signals (see Figure 9).

The control logic is comprised of simple counter and digital divider circuits. Its output is a two-phase bit clock control for the rest of the FPR electronics. The FPR start signal becomes a logical "1" every data frame, and inserts a "1" into the first stage of the 15-bit shift register (SR). Upon subsequent word clock pulses, the "1" is shifted through the 15-bit SR and toggles the flip-flop at the end. Only one stage of the SR is at logic "1" at any time and after the 15-word clock pulses, all SR stages are logic "0". The SR controls the commutator. A timing diagram is shown in Figure 10.

The purpose of the commutator is to connect, in sequence, each thermistor network to the common blocking oscillator (BO). The BO oscillation frequency is determined by the network resistance and will only operate when connected to a network.

Each RE sensor is instrumented with a separate network, as are the mounts of all sensors (RE and TF), the calibrate source and electronics package.

The sample gate, timed by the control logic, enables blocking oscillator pulses to be counted for a fixed time interval by the 10-bit counter. Upon completion of the count, each word is parallel transferred to the 7-bit SR, and read out serially. All data are transferred through the LSB transfer gates only, except for two words. The RE sensors, which cover a wide temperature range, operate the BO over a higher frequency range, and may exceed the usual 7-bit count. In the case of the two RE sensor words, the three most significant bits (MSB) of the counter are parallel transferred to the 7-bit SR in the word following the least significant bits (LSB) data for that sensor. See Table 1 for word content and formatting.

The thermal feedback (TF) system is comprised of two independent temperature control systems. The resistance of a thermistor on the sensor disk is compared with a set point resistance; the difference is converted to an error signal, which is amplified and used to control a variable frequency oscillator (VFO). The VFO in turn operates a power switch which is capacitively coupled to a heating element on the sensor disk. The switch delivers pulses of known energy at the frequency of the VFO to the heater to control the temperature so as to balance the thermistor and set point

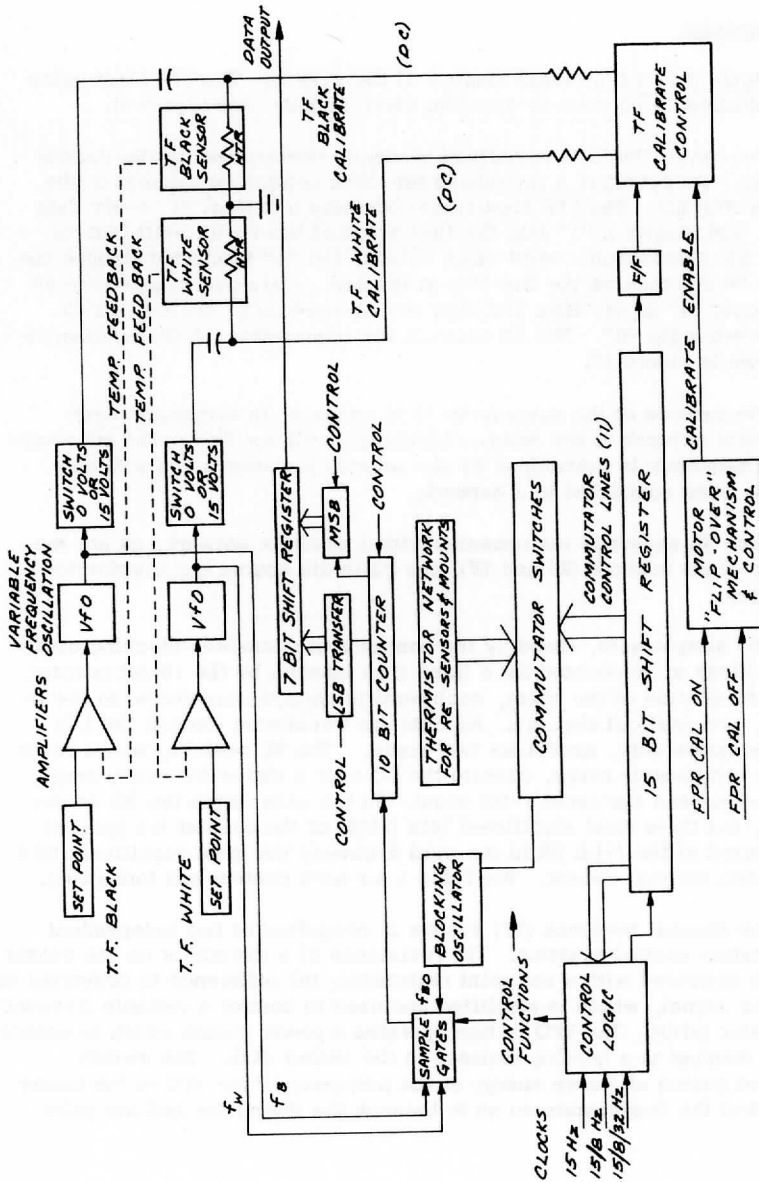
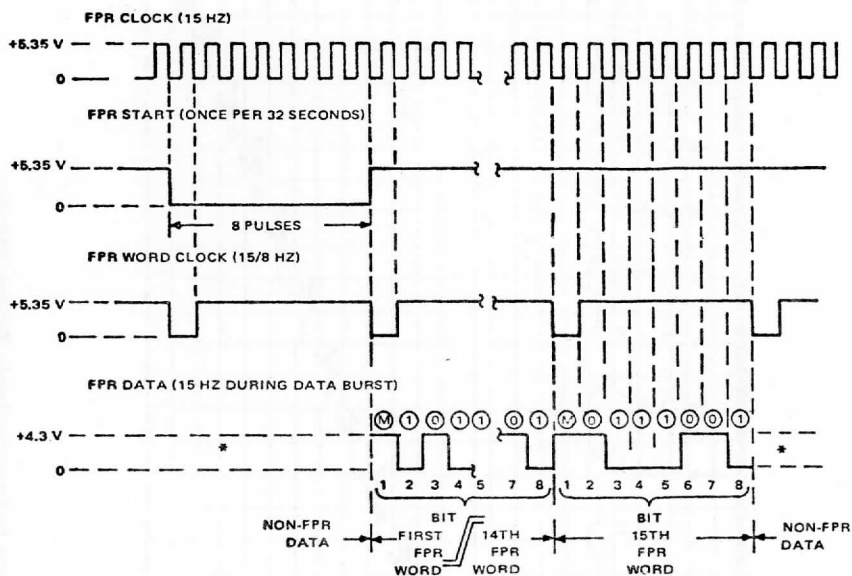


Figure 8. Flat Plate Radiometer, Function Block Diagram



## NOTES:

- \* DURING THIS PERIOD EITHER LEVEL MAY BE USED
- Ⓜ MARKER BIT (ALWAYS AT +4.3 V)
- ① LOGIC LEVEL "1" (± 0V)
- ⓪ LOGIC LEVEL "0" (+4.3 V)
- BIT 2 IS THE LEAST SIGNIFICANT BIT (LSB)
- BIT 8 IS THE MOST SIGNIFICANT BIT (MSB)
- THE DATA SHOWN IS FOR THE OUTPUT OF THE FPR,  
UPON PLAYBACK THE ORDER IS REVERSED.

Figure 9. Flat Plate Radiometer Timing Diagram. (Figure by permission of NOAA/RCA.)

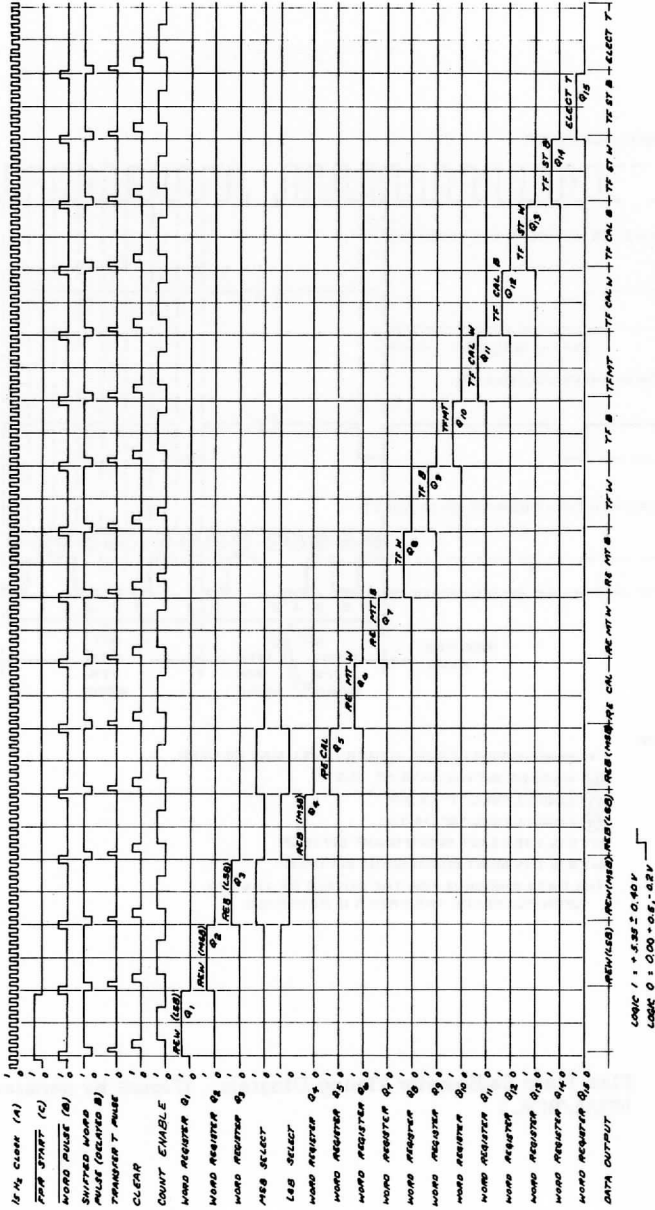


Figure 10. Flat Plate Radiometer Logic Timing Diagram



Table 1. FPR Word Content

FPR Channel No.	Secondary Sensor Subsystem Channel No.	Function	Bit Weight							
			Bit Position in Word							
(As recorded in satellite)			1	2	3	4	5	6	7	8
1	7	RE White Data	M	1	2	4	8	16	32	64
2	8	RE White Data and Flag	M	128	256	512	*	*	*	F
3	9	RE Black Data	M	1	2	4	8	16	32	64
4	10	RE Black Data and Flag	M	128	256	512	*	*	*	F
5	11	RE Calibrate**	M	1	2	4	8	16	32	64
6	12	RE Mount Temp White	M	1	2	4	8	16	32	64
7	13	RE Mount Temp Black	M	1	2	4	8	16	32	64
8	14	TF White Data	M	1	2	4	8	16	32	64
9	15	TF Black Data	M	1	2	4	8	16	32	64
10	16	TF Mount Temp	M	1	2	4	8	16	32	64
11	17	TF White Cal Source	M	1	2	4	8	16	32	64
12	18	TF Black Cal Source	M	1	2	4	8	16	32	64
13	19	TF White Surface Temp	M	1	2	4	8	16	32	64
14	20	TF Black Surface Temp	M	1	2	4	8	16	32	64
15	21	Electronics Temp	M	1	2	4	8	16	32	64

## Notes:

M denotes a marker bit (always a logic "0" level).

F denotes a flag bit to designate the state of the TF calibration rotator (a "0" denotes the sensor is in the earth-view or data-state; a "1" denotes it is in the internal hemisphere or calibrate state).

\* Denotes a not used bit (should always be at a "0").

\*\* Only the seven LSB bits are telemetered; 128, 256, 512 are not telemetered.

resistances, and maintain the sensor disk at constant temperature. The radiant energy exchange of the sensor can be determined from the pulse frequency of the heater control. The frequencies (fw and fb of Figure 8) are gated in turn to the counter and counted, etc., in the same fashion as the blocking oscillator data.

Referring again to Figure 8, when an "FPR CAL ON" command is received, a torque motor actuator "flips" the TF sensor pair 180° to view a pair of calibration targets. The F/F, which is toggled by the SR last stage, toggles the TF calibrate control to alternate states for alternate data frames. In one case, the TF calibrate control supplies DC power to the heater of each TF sensor, which results in a drop in the pulse power required to maintain the sensor temperature and thus a drop in the pulse rate. The decrease in pulse power should exactly equal the DC power if the electronics system is operating properly. If not, a system change is indicated, but may be corrected for by knowledge of the error. In the other case (no DC), with the sensor viewing a known temperature black body (the calibrate target), the pulse count change is noted. The energy exchange equation can be used to calculate the effective emissivity of the sensor and determine if changes have occurred.

More detail is given in the circuit diagrams of Figures 11 through 14 for the four circuit boards which comprise the electronics system.

## 2. Accuracy and Stability

### a. Thermal Feedback System

Stability of the TF system was determined by the temperature effects and long-term drift of the TF null detector circuitry. The closed-loop gain of the circuit can be expressed as:

$$G = K \left( \frac{A}{A\beta + 1} \right)$$

where A is the open loop gain of the amplifier. The 7-bit TF data has resolution of one part in 128. The accuracy requirement was assumed to be at least as good as the readout resolution, i. e., 1/128. This, then, requires the ratio

$$\frac{A}{1 + A\beta}$$

to be stable to one part in 128. Tests were conducted to verify a stability of one part in 150. This criterion was satisfied as long as the open loop gain A was sufficiently high. Parts were individually selected to achieve this goal.

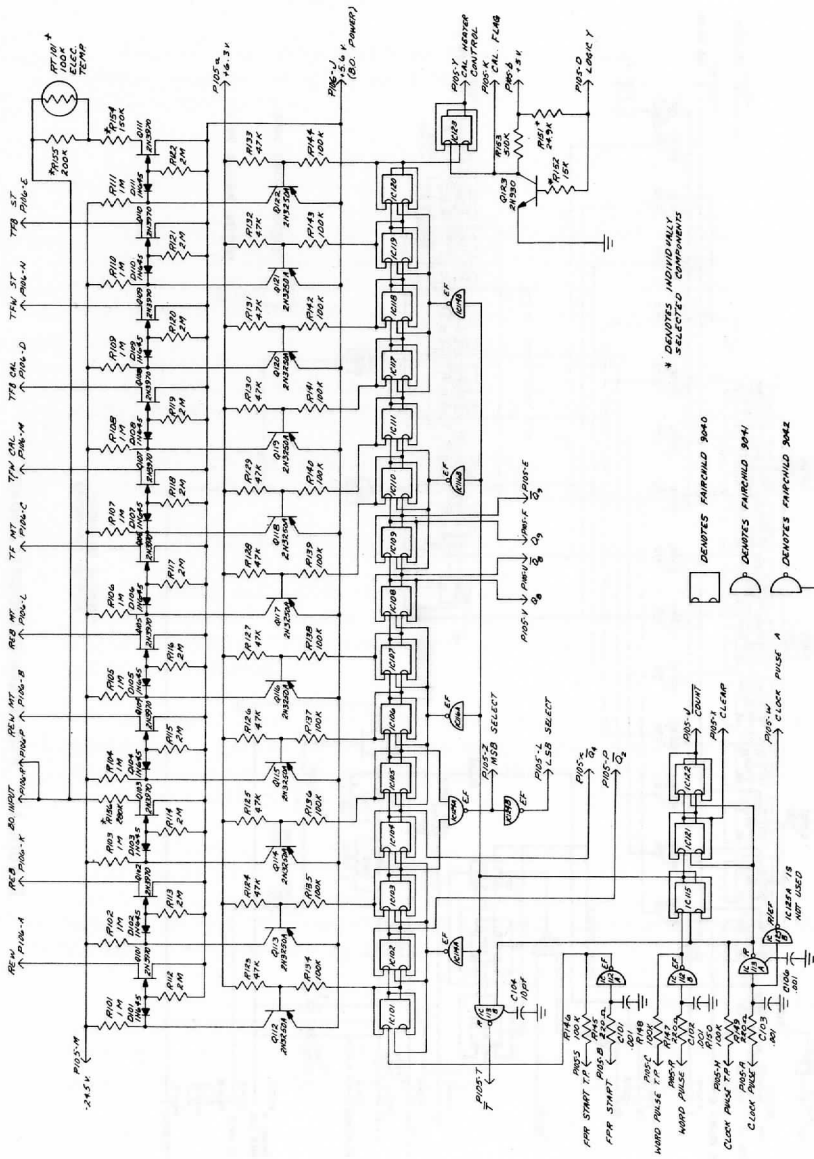
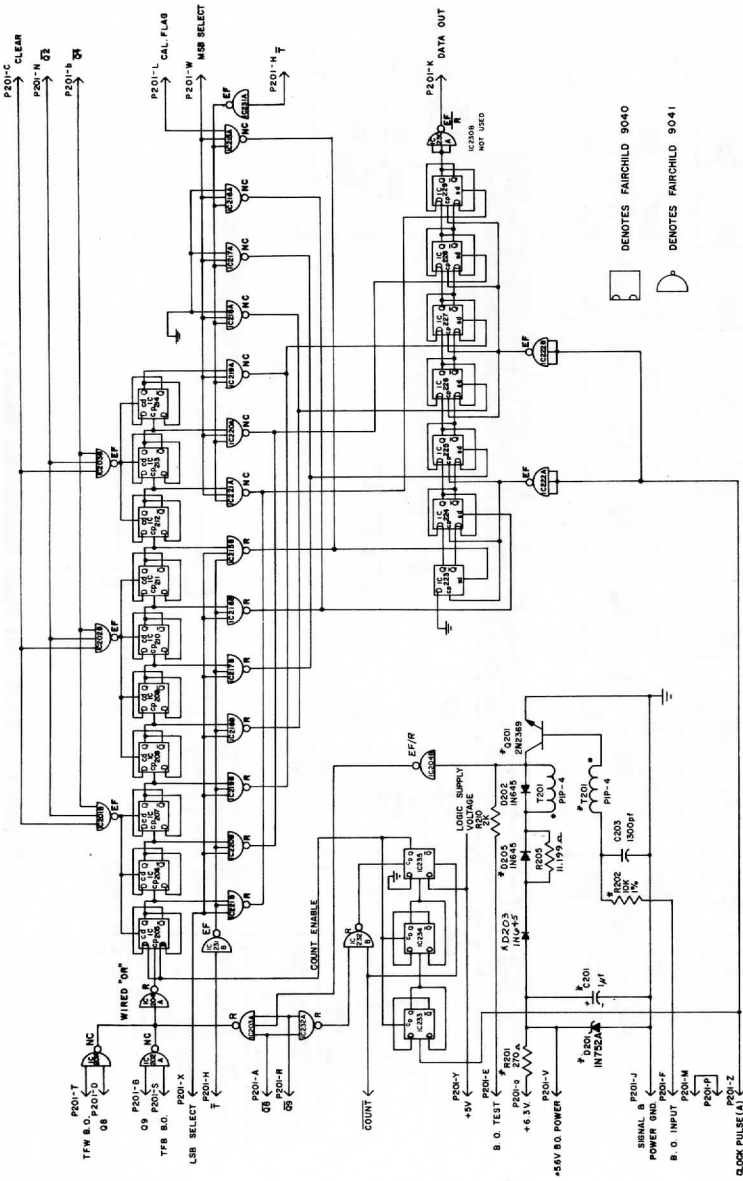


Figure 11. ITOS Flat Plate Radiometer Board 1.



\* DENOTES INDIVIDUALLY  
SELECTED COMPONENTS

Figure 12. Flat Plate Radiometer Board 2

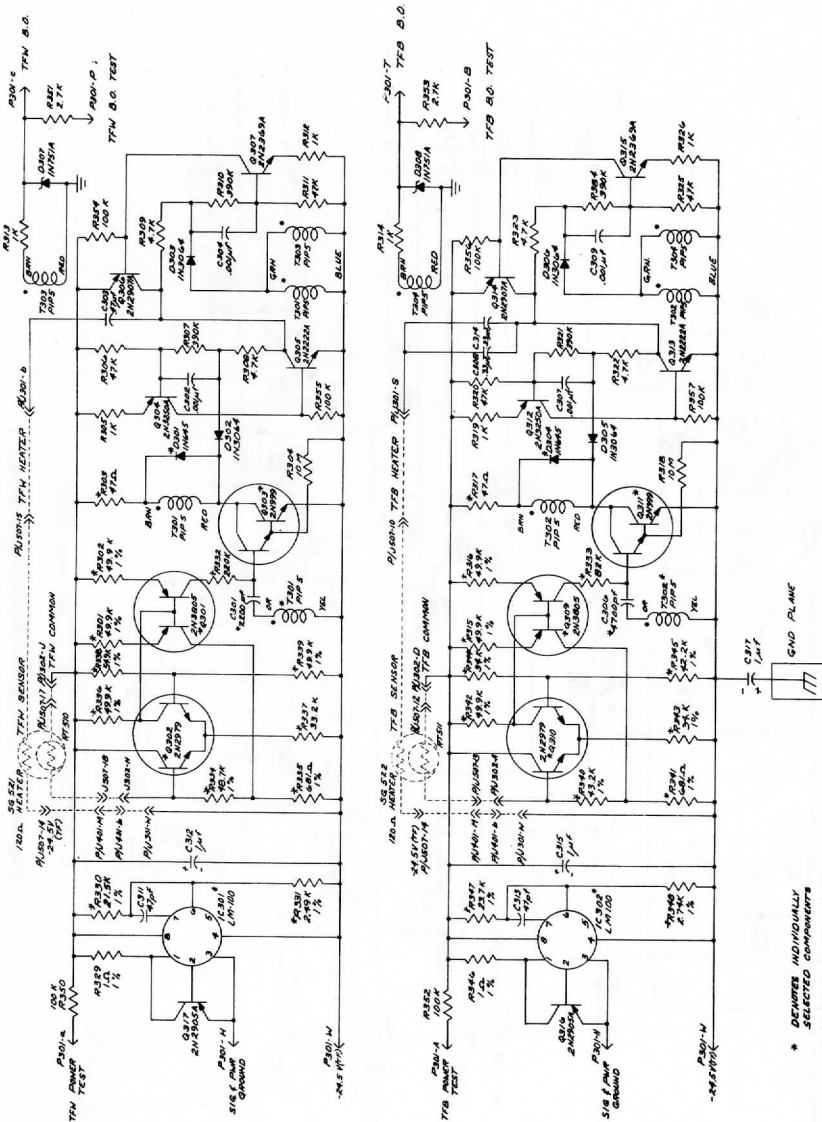


Figure 13. Flat Plate Radiometer Board 3

\* DENOTES INDIVIDUALLY  
SELECTED COMPONENTS  
..... DENOTES CIRCUITRY  
EXTERNAL TO BOARD 3

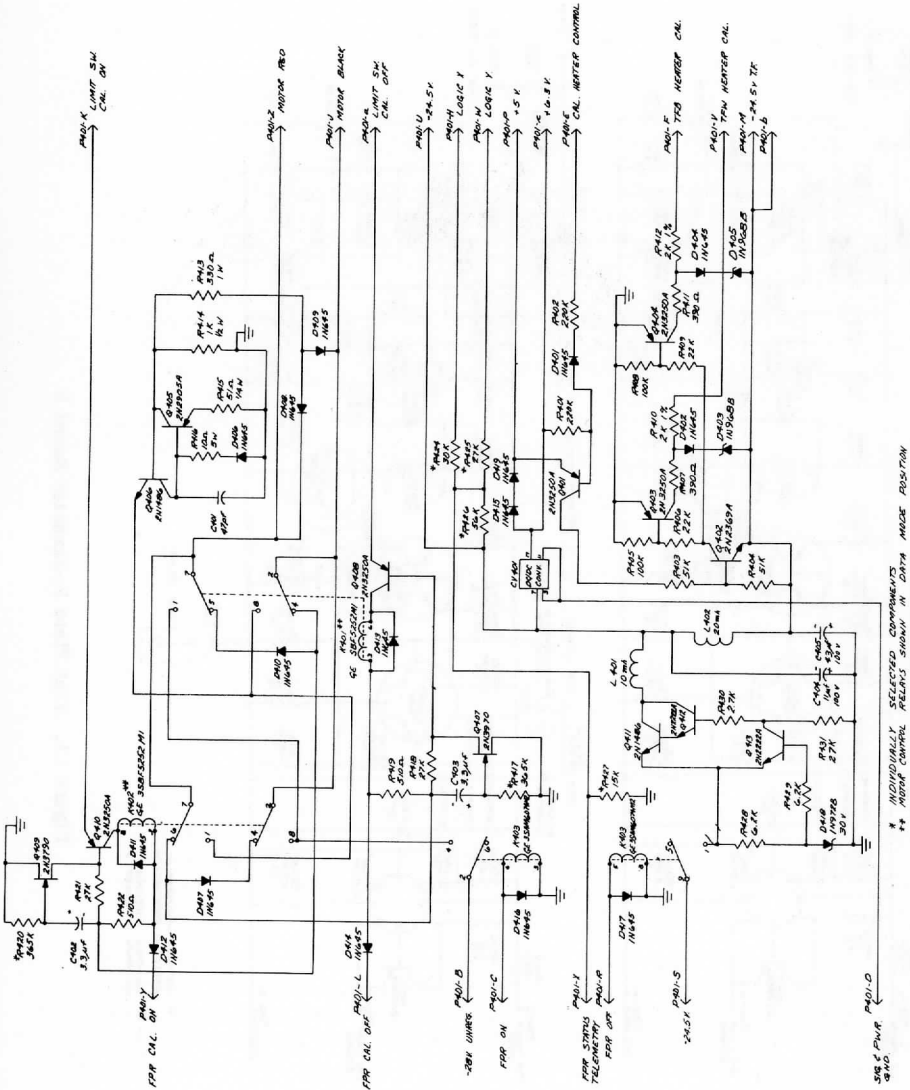


Figure 14. Flat Plate Radiometer Board 4

### b. Blocking Oscillator

Each BO was individually temperature-tested and compensation provided to maintain stability to at least one part in 1024, the resolution of the RE sensor system.

### 3. Power

Electrical power to the instrument was provided on both the regulated -24.5 VDC and the unregulated -28 volt supplies. Power to the calibrate motor drive circuit was provided by the unregulated line, all other instrument power was provided via the -24.5 VDC regulated line.

Average power required by the FPR was slightly less than 1 watt from the regulated -24.5 VDC supply. Actual power varied by about 100 milliwatts, depending on the frequency of the TF circuit pulsing.

Power from the unregulated -28 V supply was used only for the calibrate motor drive and was about 2 watts peak with a duration less than one second.

### Reliability and Components

No formal reliability and quality assurance requirements were imposed for the program. However, "Inspection System Provisions for Suppliers of Space Materials, Parts, Components and Services," NPC 200-3, was generally followed.

Informal Failure Mode Effectivity, Criticality Analysis (FMECA) was performed as part of the design process. Major consideration for failure effects was the impact of possible FPR failure on the spacecraft via the FPR electrical interface.

All soldering and assembly was performed by NASA-qualified personnel, according to NPC 200-4, "Quality Requirements for Hand Soldering of Electrical Connections." Assembly and tests were performed according to written procedures. Temperature tests and vacuum operations were performed on both subsystem and system level.

Parts for use in the FPR were selected from the GSFC PPL-9 and the RCA Preferred Parts List wherever possible. Nonstandard parts were subjected to extra screening, performed both in-house and by the vendor. Nonstandard parts were justified by prior spaceflight use, wherever possible.

All logic elements were from the Fairchild 9040 family.

#### 4. RFI and Compatibility

The controlling document for spacecraft/instrument compatibility was the FPR Subsystem Interface Specification. All input logic lines at the interface were filtered with RC networks (Figure 11). Power turn-on di/dt requirements were met by filtering with a two-stage LC network. Further detail can be seen by referring to Figure 14, ITOS FPR Board 4 Electrical Schematic.

#### 5. Modifications to S/N 005 FPR

One unit, S/N 005, carried a set of cone shielded RE sensors in place of the TF sensors. Modification of the electronics was required to accommodate this change. Since S/N 005 FPR was mounted on ITOS-B which failed to achieve orbit, these modifications are not included here. For a discussion of the S/N 005 system, the reader is referred to "ITOS Meteorological System, ITOS-B; Final Engineering Report," published by RCA/AED.

### D. MECHANICAL DESIGN

#### 1. Physical Requirements

##### a. Mechanical Interface

- 1) Outline: The unit conforms to the outline dimensions specified in Figure 15, Flat Plate Radiometer Outline Drawing.
- 2) Mounting: The unit is mounted directly to the spacecraft by means of four 1/4-28 bolts which mate with four self-locking nuts fastened within the FPR baseplate. The hole pattern is specified in the outline drawing.
- 3) Weight: The maximum weight for the unit is 5.5 pounds.

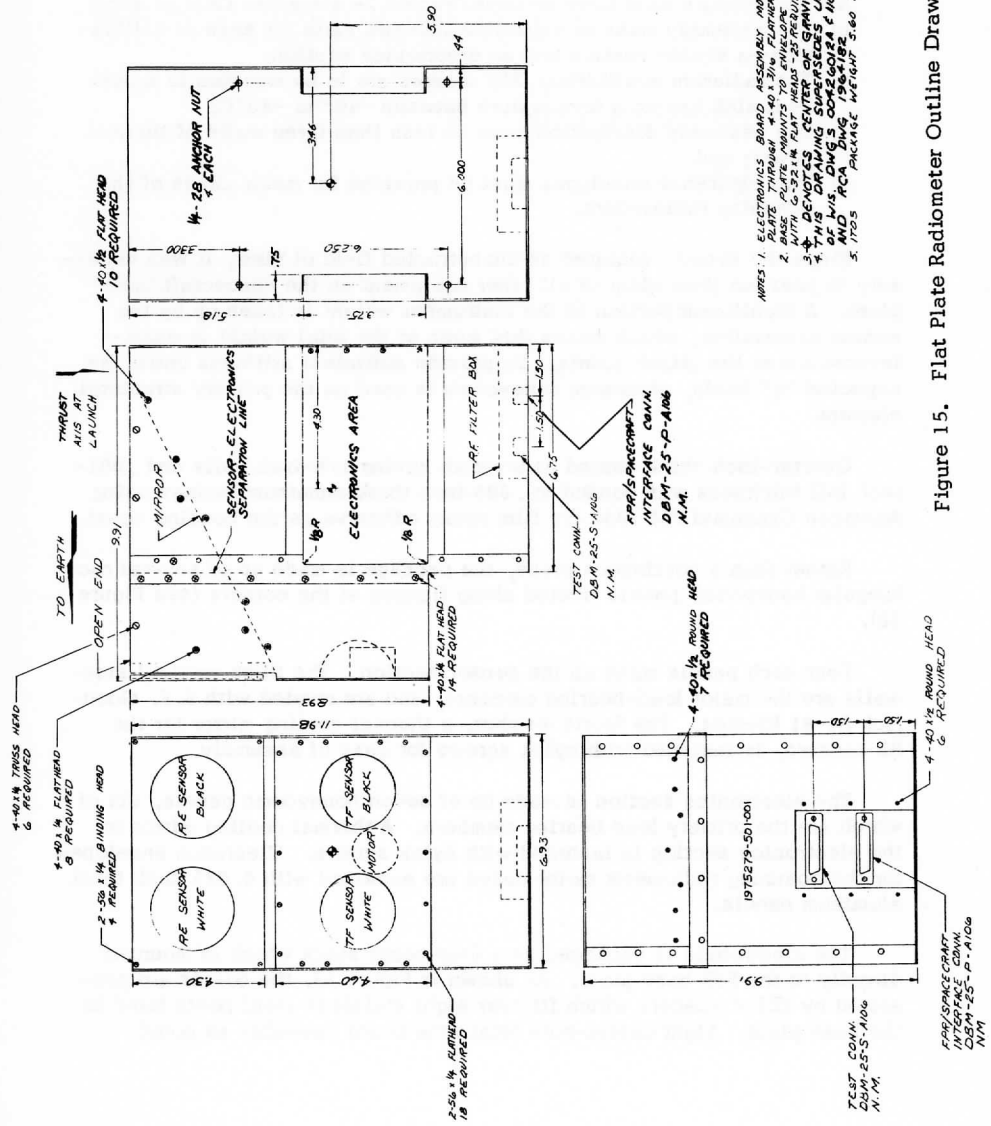
##### b. Electrical Interface

The location of the electrical interface and test connector is as noted on the outline drawing.

##### c. Design Environment

The vibration and thermal-vacuum design environments are specified in RCA Drawing 1750920, Subsystem Environmental Test Specification for TOS Systems.





- NOTES: 1. ELECTRONICS BOARD ASSEMBLY MOUNTS TO BASE PLATE WITH 4-1/4\"/>
  2. BASE PLATE MOUNTS TO ENVELOPE WITH 6-32 IN. FLAT HEAD - 25 REQUIRED
  3. DETECTOR CENTER OF GRAVITY MUST BE WITHIN CENTER OF GRAVITY OF THIS DRAWING 00F50018 & 1003022A AND RCA DWG 198-1182
  5. 1705 PACKAGE WEIGHT 5.60 L.B.

Figure 15. Flat Plate Radiometer Outline Drawing

## 2. Design

The design of the package was influenced primarily by the following requirements:

- a) The sensors must have an unobstructed  $2\pi$  steradian field of view;
- b) The assembly must be separable into two parts for ease of calibration—a sensor section and an electronics section;
- c) The radiative equilibrium (RE) sensors are to be mounted to a cold heat sink having a temperature between  $-40^{\circ}$  to  $-80^{\circ}\text{C}$ ;
- d) The assembly dissipation must be less than three watts of thermal power; and
- e) Two clearance envelopes must be provided for motor cases of the scanning radiometers.

Since the sensors required an unobstructed field of view, it was necessary to position them clear of all other equipment on the spacecraft baseplate. A significant portion of the instrument weight is taken up by the sensor assemblies, which means that much of the total weight is cantilevered above the attach points. To provide sufficient stiffness under the expected "g" loads, aluminum honeycomb is used as the primary structural element.

Quarter-inch-thick vented honeycomb having 1/4-inch cells and .001-inch foil thickness was bonded to .005-inch thick aluminum facings using American Cyanamid FM 1000 dry film epoxy adhesive as the bonding agent.

Rather than a continuous piece, the package is made up of several rectangular honeycomb panels riveted along flanges at the corners (see Figure 16).

Four such panels make up the sensor section. The three vertical sidewalls are the major load-bearing members, and are riveted with B. F. Goodrich A4-81 Rivnuts. The fourth member, a thermal cooling mirror for the RE sensors, is fastened with nylok screws for ease of assembly.

The electronics section is made up of seven honeycomb panels, six of which are the primary load bearing members. A thermal cooling mirror in the electronics section is fastened with nylok screws. Clearance envelopes for the scanning radiometer motor cases are enclosed with 0.025-inch thick aluminum panels.

The electronics is packaged as a four-board stack which is mounted directly to the FPR base plate. As shown in Figure 17, the boards are separated by KEL-F spacers which fit over eight stainless steel posts fixed to the base plate. Eight castel-nuts retain the board assembly as noted.



Figure 16. Flat Plate Radiometer Instrument Package

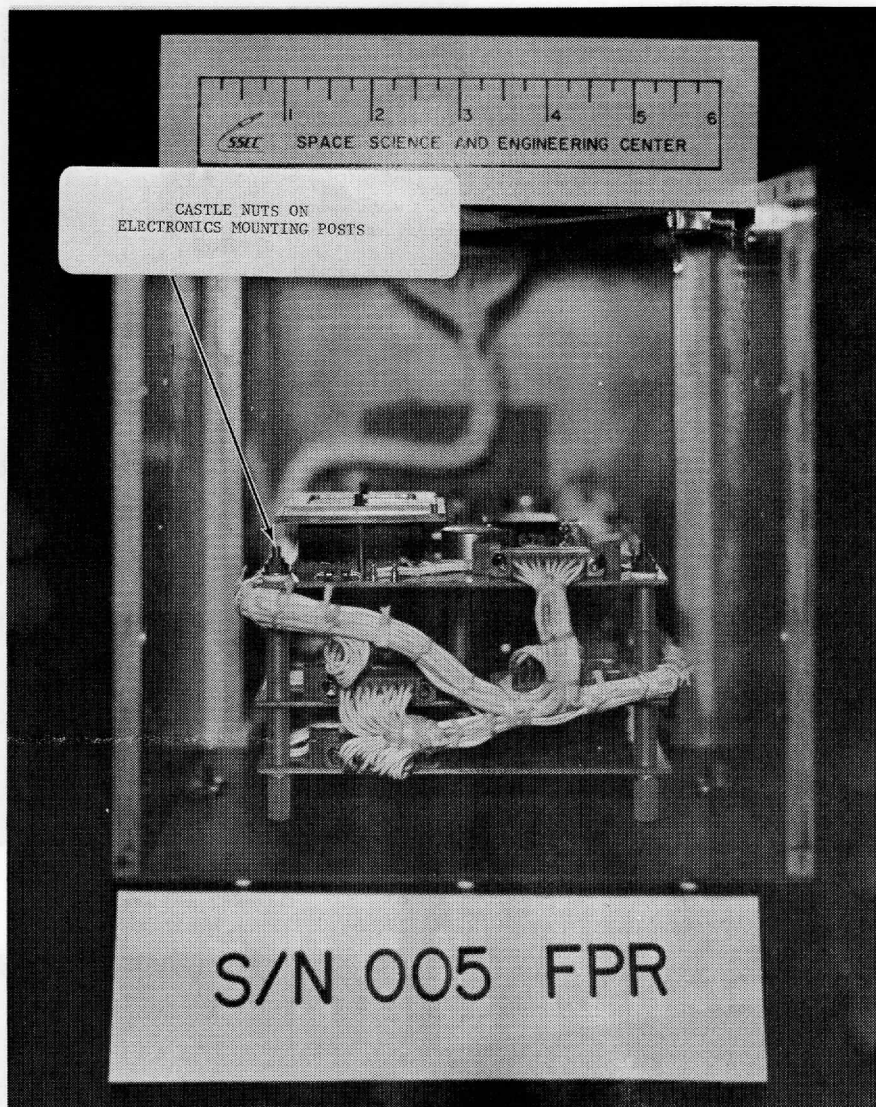


Figure 17. View of Flat Plate Radiometer Electronics

### 3. Fabrication

#### a. Honeycomb Panels

The honeycomb panels are fabricated as shown in Figure 18 from:

- 1) a lightweight magnesium frame having the desired outside dimensions,
- 2) a honeycomb core cut to fit the frame inside dimensions, and
- 3) two aluminum facings and two sheets of film epoxy cut to fit the frame outside dimensions.

The assembly is accomplished by:

- 1) clamping the components into an appropriate fixture,
- 2) heating the fixture/panel assembly to 350°F and holding for two hours,
- 3) drilling and tapping the panels as specified on the individual part drawing, and
- 4) assembling according to the appropriate assembly drawing.

#### b. Surface Finishes

All aluminum and magnesium surfaces are treated with Allied Research Products Iridite according to the manufacturers' recommended procedure.

In addition, the honeycomb panels are painted with J. L. Amritage M1207 and M1178 epoxy paint which is supplied by the spacecraft manufacturer.

## E. THERMAL DESIGN

### 1. General

The FPR instrument package was designed to provide the thermal environments necessary for efficient sensor operation while minimizing the heat loss through the instrument.

The primary objectives of the thermal design are:

- a. to provide a low temperature (-40° to -80° C) mounting surface for the RE sensors,
- b. to provide a moderate temperature (+20° to -15° C) mounting surface for TF sensors,

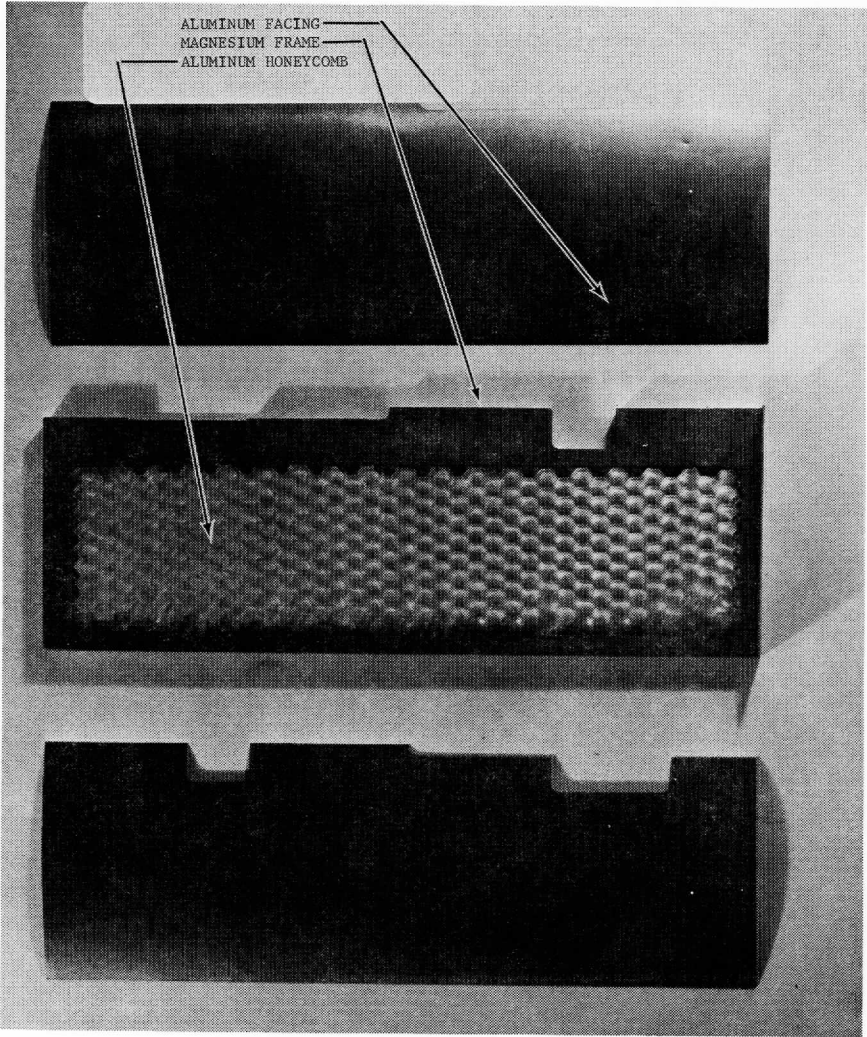


Figure 18. Honeycomb Panel Construction

- c. to maintain the electronics temperature above  $-15^{\circ}\text{C}$ , and
- d. to maintain the heat loss from the spacecraft at the spacecraft/instrument interface below 3 watts.

## 2. RE Sensor Mount

It was determined that the RE sensors operate most efficiently at very low mount temperature. To achieve the temperatures which are required, the package is configured to take advantage of radiative cooling to deep space (see Figures 1 and 19).

The design of the RE mounting plate is such that it is well decoupled from all possible sources of heat input and is tightly coupled radiatively to deep space (a cold sink).

The KEL-F thermal isolation blocks impede the flow of heat by conduction between the FPR envelope and the RE mounting plate. KEL-F was chosen because of its low thermal conductivity and good dimensional stability in a vacuum environment.

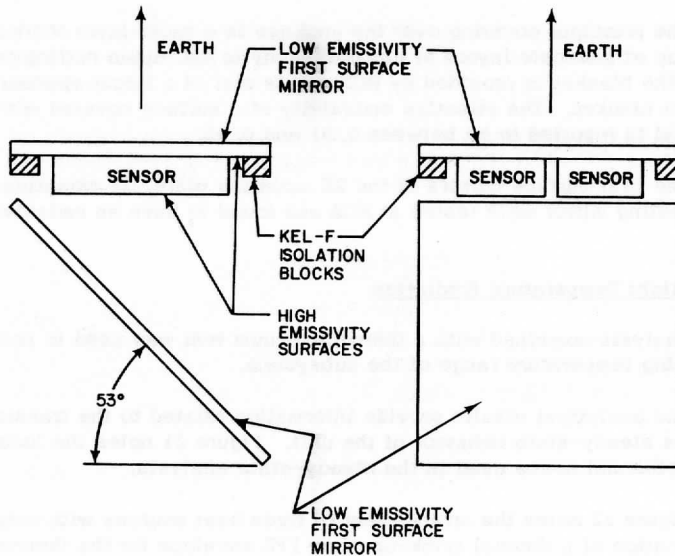


Figure 19. RE Sensor-Cooling Mirror Geometry



Infrared radiation from the high emissivity back surface of the mounting plate is reflected to deep space. A mirror angle of  $53^\circ$  was chosen to prevent earth radiation from reaching the rear of the RE mounting plate by reflection from the mirror.

### 3. TF Sensor Mount

In order to maintain the TF mounting surface at a reasonable temperature, it is necessary to provide a high conductance path between the spacecraft and the TF plate. This path, primarily conductive through the honeycomb facings and magnesium framework of the envelope, also minimizes gradients within the package.

### 4. Spacecraft Heat Loss

All external surfaces of the FPR with the exception of the RE mounting plate rear surface have a low effective emissivity due to surface finish or thermal blanket cover. In this way it is possible to isolate the package from its surroundings and minimize the heat loss from the spacecraft through the FPR.

The principal covering over the package is a multi-layer thermal blanket made up of alternate layers of aluminized mylar and nylon netting (see Figure 20). The blanket is provided by RCA and is part of a larger spacecraft thermal blanket. The effective emissivity of a surface covered with this material is reported to be between 0.01 and 0.02.

The first surface mirrors of the RE mounting plate, TF mounting plate and cooling mirror were tested at RCA and found to have an emissivity of 0.05.

### 5. Flight Temperature Prediction

Analysis combined with a thermal-vacuum test was used to predict the operating temperature range of the subsystem.

The analytical results provide information related to the transient as well as steady-state behavior of the unit. Figure 21 notes the location of the isothermal nodes used in the steady-state analysis.

Figure 22 notes the arrangement of three heat sources with respect to the location of a thermal mock-up of an FPR envelope for the thermal vacuum test. The test was designed to simulate several of the expected in-flight environments.



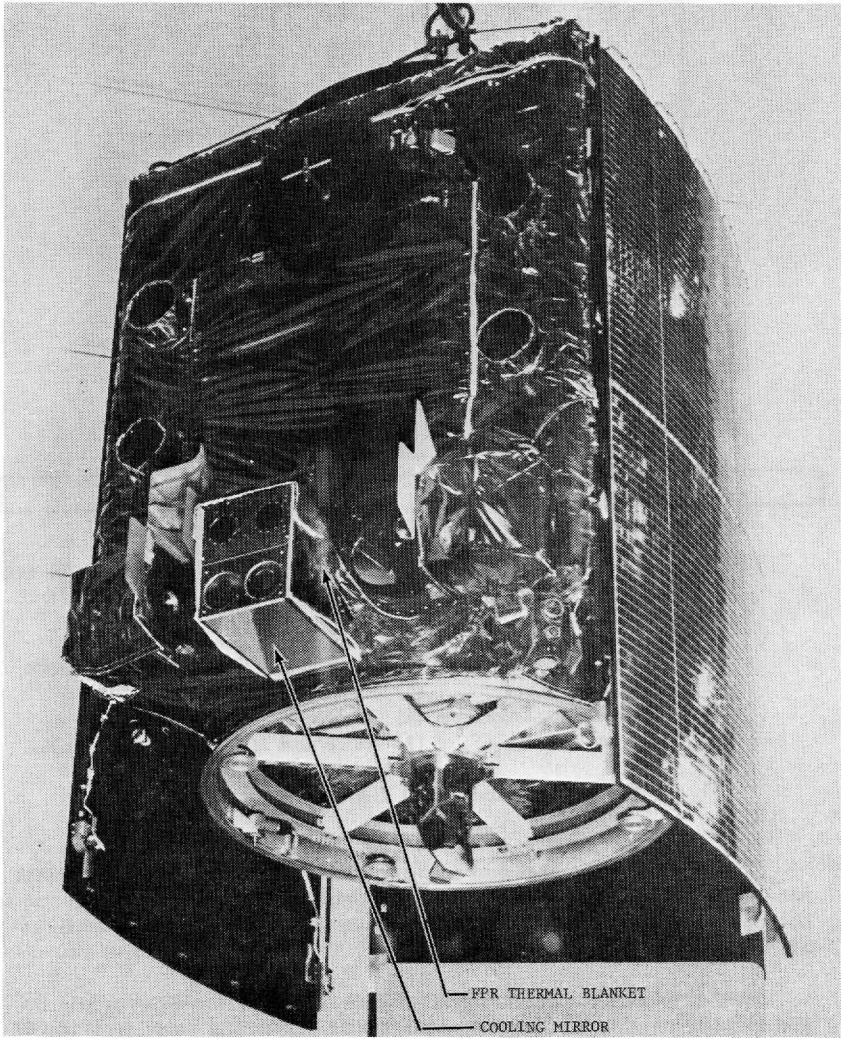
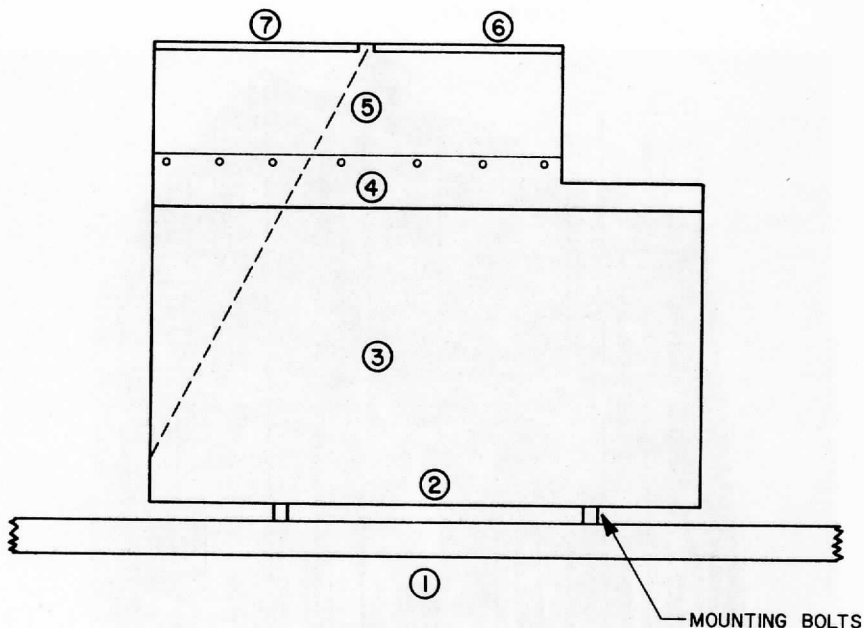


Figure 20. Flat Plate Radiometer Mounted on Spacecraft

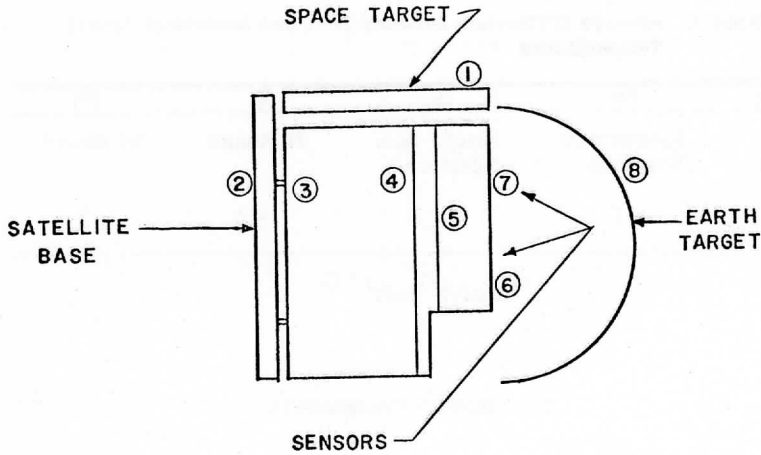


- |                          |                                      |
|--------------------------|--------------------------------------|
| (1) Space Craft Base     | (4) Electronics/Radiometer Interface |
| (2) FPR Base Plate       | (5) Radiometer Envelope              |
| (3) Electronics Envelope | (6) TF Mount                         |
|                          | (7) RE Mount                         |

Figure 21. Analytical Thermal Schematic

The results of the test and a comparison of analytic and test results are tabulated in Tables 2 and 3. A reasonable degree of correspondence is noted. More importantly, the results indicate the package temperatures are within the system requirements.

Further transient analysis predicted that the FPR envelope would be stable within  $\pm 1.0^\circ \text{C}$  over a typical orbit while in the same orbit the RE mounting plate would be stable within  $\pm 3.0^\circ \text{C}$ . Tabulated values for one RE mount survey are included in Table 4.



- |  |                                      |
|--|--------------------------------------|
| (1) Liquid Nitrogen Target                   | (5) Electronics—Radiometer Interface |
| (2) Satellite Base Plate                     | (6) TF Mount                         |
| (3) FPR Base Plate                           | (7) RE Mount                         |
| (4) Electronics Package<br>(honeycomb panel) | (8) Earth Target                     |

Figure 22. Thermal Vacuum Test Set-up

Table 2. Thermal Vacuum Data Summary

(2)	(3)	(4)	(5)	(6)	(7)
Spacecraft Base	FPR Base	Electronics Envelope	Elect. -Rad. Interface	TF Mount	RE Mount
-0.7	-0.1	-2.3	-2.4	-	-59.0
+7.2	5.8	2.6	0.6	0.8	-56.5
15.0	13.4	10.1	7.8	-	-50.7
20.1	18.0	14.2	-	11.4	-50.2
30.1	26.2	21.9	16.9	-	-46.1
34.9	30.4	25.4	-	21.0	-44.8

Temp. °C

Table 3. Average Difference Between Test and Analytical Model Temperatures

(3)	(4)	(5)	(6)	(7)
FPR Base	Electronics Envelope	Elect. -Rad. Interface	TF Mount	RE Mount
$\pm 1$	$\pm 1$	$\pm 2$	$\pm 2$	$\pm 3$

$$(T_{\text{analyt}} - T_{\text{test}}) \text{ } ^\circ \text{C}$$

## F. SENSOR CALIBRATION

### 1. In-Air Calibration

The purpose of the in-air calibration is to determine the relationship between thermistor output\* (blocking oscillation counts) and temperature over the expected range of sensor temperatures.

The calibration is conducted in a thermally controlled chamber which is well-instrumented to confirm that near isothermal conditions prevail. A description of the calibration chamber can be found in the TIROS-M FPR Calibration Report CR-1, paragraph 2.1. The procedure followed for the tests is outlined in TP-1-A, TIROS-M/TIROS FPR Test Procedure.

Raw calibration data is recorded automatically on printer tape during a calibration. The information is recorded as a data frame which is made up of 15 FPR words and eight temperatures. During a typical calibration, approximately 2000 frames are recorded over a temperature range between  $-80^\circ \text{C}$  to  $+100^\circ \text{C}$ .

Several adjustments must be made to the data by computer, in accordance with the FPR calibration Data Handling Procedure, and then plotted. Only two of these adjustments actually modify the data count. The first applies a correction for a jumper cable between the electronics and sensor sections which tends to lower the total count. The second correction takes

---

\* This calibration applies to all FPR words except the RE calibrate, TFW, TFB, and electronics temperature.

Table 4. Calculated RE Mount Transient Temperatures

Orbit Position* (deg.)	Earth Radia- tion W/sq. M	Albedo W/sq. M	Direct solar W/sq. M	Earth temp (B. B.) (° K)	FPR Envelope temp (° K)	RE Mount (° K)
0	137.7	245.0	0.0	286.6	270.0	188.1
15	142.7	245.0	0.0	287.5		187.6
30	147.9	245.0	0.0	288.5		187.2
45	132.0	268.0	0.0	289.8		186.8
60	110.2	315.0	0.0	294.2		186.6
75	110.2	420.0	0.0	310.9		186.9
90	110.2	490.0	0.0	320.7		187.4
105	110.2	0.0	257.0	283.6		186.9
120	110.2	0.0	496.0	321.5		187.5
135	132.8	0.0	700.0	348.1		189.0
150	147.9	0.0	860.0	365.1		191.2
165	142.7	0.0	0.0	223.9		189.3
180	137.7	0.0	0.0	221.9		187.6
195	137.7	0.0	0.0	221.9		186.0
210	147.9	0.0	860.0	365.1		188.5
225	164.2	0.0	700.0	351.3		190.1
240	170.0	0.0	496.0	329.2		190.7
255	175.8	0.0	257.0	295.5		190.1
270	158.6	490.0	0.0	327.0		190.6
285	175.8	420.0	0.0	320.1		190.8
300	170.0	315.0	0.0	304.1		190.5
315	167.1	268.0	0.0	295.9		190.0
330	147.9	245.0	0.0	288.5		189.3
345	147.9	245.0	0.0	288.5		188.7
360	137.7	245.0	0.0	286.6		188.1

\* 0 = subsatellite point at equator

into account any changes in the RE calibrate word which in turn reflects electronics drift. A typical computer plotted in-air calibration curve is shown in Figure 23.

## 2. Vacuum Calibration

Because the TF sensor is an active detector which dissipates a significant amount of power on its sensitive surface, it must be calibrated in-vacuum to make a meaningful heat balance measurement. Calibration procedure is given in paragraph 2.2 of CR-1, TIROS-M FPR Calibration Report.

Like the in-air calibration, the data from the vacuum calibration must be adjusted. The adjustments are described in the FPR Calibration Data Handling Procedure. A typical computer plot of final unsmoothed vacuum calibration data is shown in Figure 24. Note the effect of mount temperature on sensor response. (The apparent jitter in the data is due largely to the  $\pm 1$  count in quantization with 7 bits.)

## 3. RE Loss Measurement

The in-air calibration of the RE sensors does not represent a complete calibration of the detector since it does not take into account any thermal losses between the sensor and its mount (the in-air calibration is performed under near-isothermal conditions). In flight, a temperature difference of 150° C between the sensor and mount is not uncommon. It is necessary, therefore, to make a correction for the thermal coupling between the sensor and mount. Correction factors as determined from test and analysis are provided for each subsystem.

# G. PERFORMANCE AND RESULTS

## 1. Operation Summary

Five FPR subsystems were delivered under the contract. The allocation and performance of the units are summarized in Table 5.

As noted, only two units have been orbited and used operationally. Both of these units have performed normally. Termination of operation was the result of failure in the spacecraft data handling system rather than any malfunction of the FPR's.

Table 5. FPR Unit History Summary

Unit	Spacecraft	Launch	Last operation	S/C deactivated
S/N001	Engrg. Test Model			
S/N002	ITOS-A → NOAA-1	12/11/70	5/28/71(1)	8/19/71
S/N003	TIROS-M → ITOS-1	1/23/70	11/17/71(1)	6/16/71
S/N004	ITOS-C(4)			
S/N005(2)	ITOS-B	10/25/71(3)		

- (1) Termination due to failure of Incremental Tape Recorded (ITR) on spacecraft, not due to FPR failure.
- (2) Cone shielded RE sensors replacing TF sensors.
- (3) Failed to achieve orbit.
- (4) Mounted on ITOS-C in flight readiness.

## 2. Results

The results from a typical orbit of operation are shown in 26.

The data is what one would expect. For these curves the count from the data system is plotted rather than temperature or irradiance, etc., since this is the basic system output. Conversion to actual parameters is done by computation later. In order to indicate typical ranges in parameters, a few values are given on the curves. The abscissa of the curves is given in data frames; a data frame is produced every 32 seconds. Thus, the abscissa represents time along the orbit path.

### a) RE Data

Starting at the left-hand side of Figure 25, the spacecraft is on the sunlit side of the earth but the sensors are shielded by the spacecraft and receive only reflected solar and long-wave radiation. However, when the spacecraft passes over the terminator, the sensors begin to be exposed to

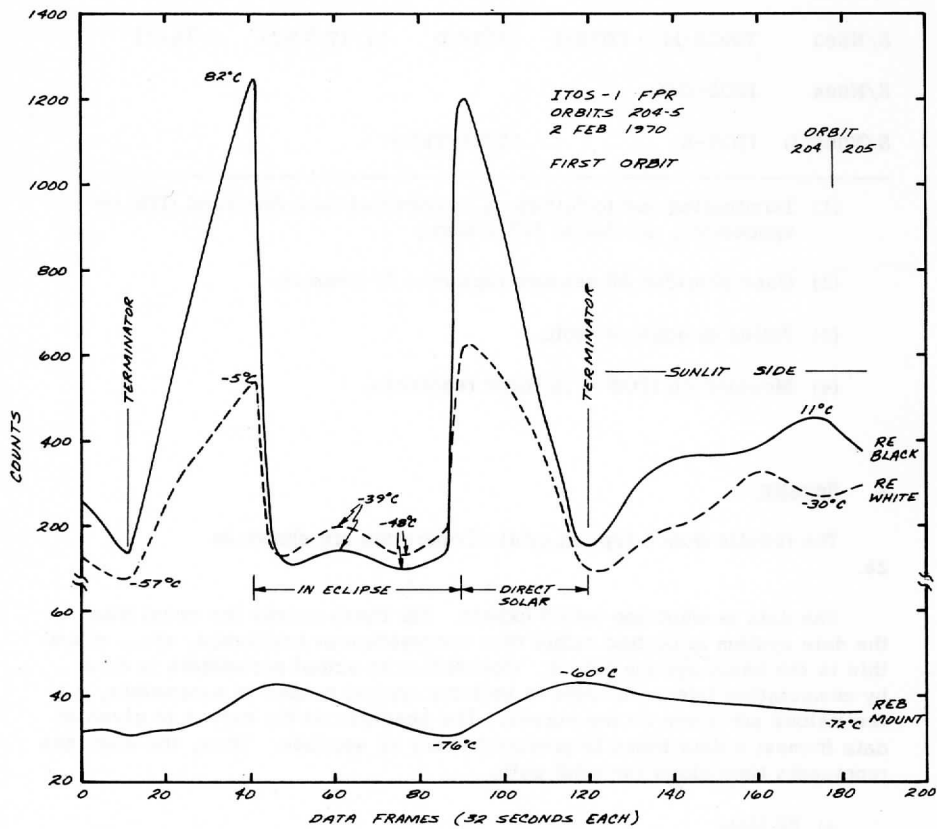


Figure 23. Typical RE Sensor In-Air Calibration Data Plot



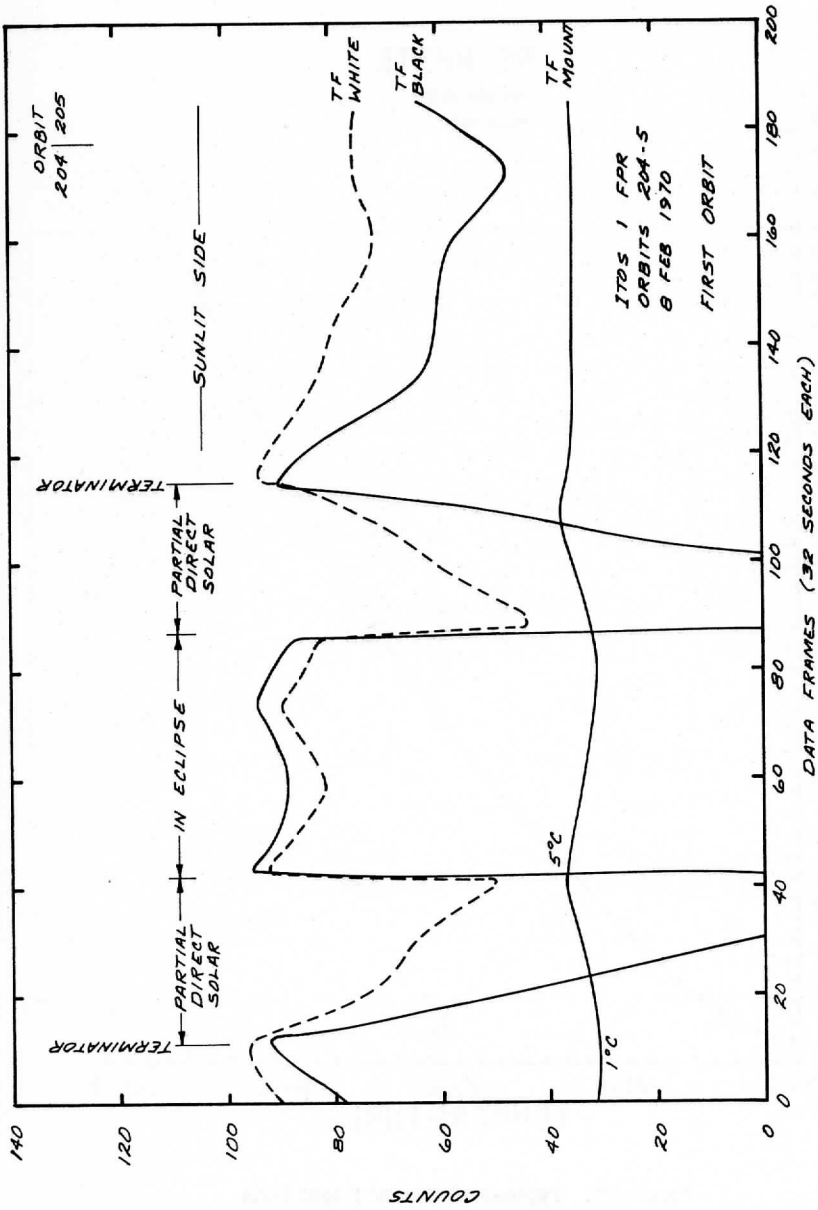


Figure 24. Typical TF Sensor Vacuum Calibration Data Plot

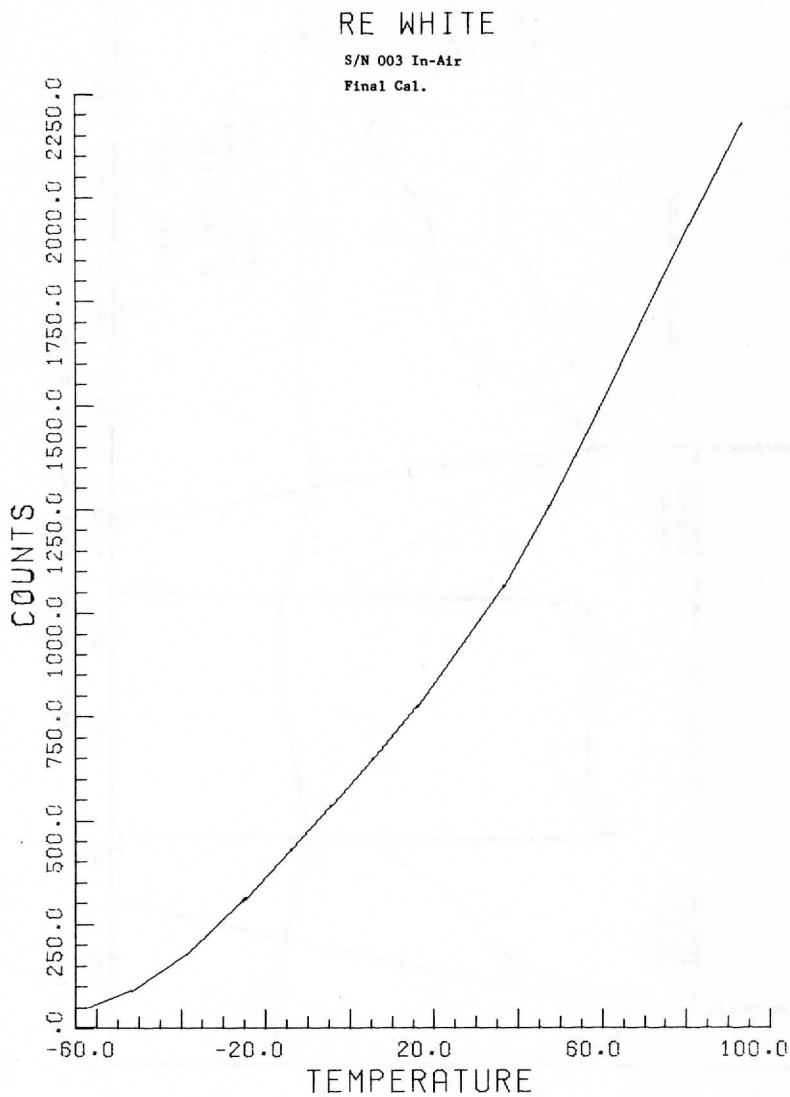


Figure 25. Typical RE Sensor Flight Data

FPR S/N 004 TF BLACK

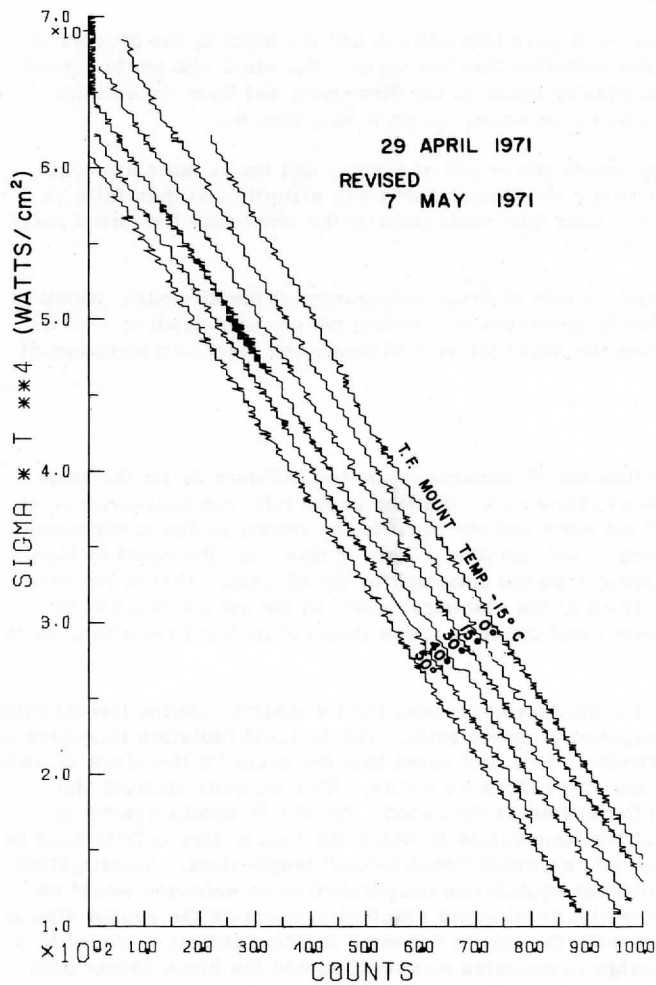


Figure 26. Typical TF Sensor Flight Data

direct solar which reaches a maximum just before the spacecraft goes into eclipse (see Figure 3). At the maximum the direct solar component has a magnitude of about one-half solar constant. As indicated the maximum equilibrium temperature is about  $80^{\circ}\text{C}$  for the black sensor but only  $-5^{\circ}\text{C}$  for the white sensor which reflects most of the solar.

The spacecraft next goes into eclipse and the input to the sensors is now only long-wave radiation from the earth. The black and white sensor should look about equally black on the long-wave and have essentially the same equilibrium temperature, which in fact they do.

When the spacecraft comes out of eclipse and the sensors are again exposed to direct solar, the temperature rises abruptly and then falls as the amount of direct solar decreases until at the terminator the direct solar goes to zero.

It is interesting to note that the temperature of the RE mount, which is cooled by radiation to space via the cooling mirror, gets down to  $-76^{\circ}\text{C}$  during eclipse when the heat load is a minimum and reaches a maximum of only  $-60^{\circ}\text{C}$ .

#### b) TF Data

Typical data from the TF sensors is plotted in Figure 26 for the same orbit as the RE data of Figure 25. Starting at the left, the spacecraft is on the sunlit side of the earth and the input to the sensor is due to reflected solar and earth long-wave radiation. Note in this case the count is high and the curves appear inverted compared to the RE case. This is because the count is a measure of the electrical power to the sensor required to keep the total power input constant rather than the incident radiation, as in the RE case.

Again, when the spacecraft crosses the terminator, moving toward eclipse, the sensors are exposed to direct solar. The incident radiation increases and so the count decreases. One now notes that the count for the black TF sensor goes to zero and stays there for a time. This happens because the dynamic range of the system is exceeded. For the TF sensor system to remain operational the temperature at which the sensor disk is held must be higher than the highest expected "equilibrium" temperature. Investigation showed that the highest equilibrium temperature to be expected would be about  $100^{\circ}\text{C}$ . The electrical power required to maintain the sensor disc at such a temperature with the lowest expected incident radiation proved to be prohibitive. A design compromise was reached and the black sensor disk temperature was set at  $50^{\circ}\text{C}$  and the white disk at  $40^{\circ}\text{C}$ . Hence, whenever the equilibrium temperature of the disk exceeds the control temperature, no electrical power is required and the count remains at zero. (The maximum

black disk temperature in this case was 79° C, compared with an RE temperature of 82° C.)

The spacecraft then goes into eclipse and both sensors receive only long-wave radiation and should track each other, which they do. The rest of the orbit follows as in the case of the RE sensors.

The mount temperature is also plotted and is seen to run from 1° C to 5° C. This temperature is influenced strongly by the spacecraft baseplate temperature so these values are not too significant.

### 3. Data Reduction and Analysis

All data collection and data reduction is the responsibility of the National Oceanic and Atmospheric Administration.